π-Strain-Induced Electrophilicity in Small Cycloalkynes: A DFT Analysis of the Polar Cycloaddition of Cyclopentyne towards Enol Ethers

Luis R. Domingo,*[a] Patricia Pérez,[b,c] and Renato Contreras[c]

Keywords: Cycloadditions / Cycloalkynes / Density functional calculations / Electrophilicity / Strain

Small cycloalkynes possess a π-strain-induced electrophilicity related to the bending of the C^{sp^3}–C^{sp}–C^{sp} bond angle. For cyclopentyne and benzyne, the electrophilicity index defined in the context of density functional theory gives a coherent rationale for the reactivity of these cycloalkynes, which may act as electrophiles in polar cycloaddition reactions toward enol ethers.

Introduction

Small-ring cycloalkynes continue to be a source of intense experimental and theoretical studies. Gilbert has reported an experimental study on the pericyclic [2+2] and [4+2] cycloadditions of several cycloalkynes, including cyclopentyne (**1**), with alkenes and enol ethers. The [2+2] process of cyclopentyne is completely diastereoselective when stereochemically labeled alkenes are used (see Scheme 1).[1,2] This result, which could be taken as a signal for a concerted mechanism, is, however, inconsistent with the principle of conservation of orbital symmetry[3] in pericyclic processes.[4] An alternative mechanism was therefore proposed by Gilbert et al. to account for this outcome.[5] The key to this mechanism is that the [2+2] cycloadduct **3** is formed by a stereospecific ring expansion of the spirocyclopropylcarbene **2**, derived from a [1+2]-allowed cycloaddition of cyclopentyne to the alkene (see Scheme 2).[5] Norbornyne (**4**) has also been used in pericyclic reactions with alkenes.[6] However, a more complex product distribution was obtained when **4** was allowed to react with dihydropyran (**5**), a result probably associated with the norbornane chemistry (see Scheme 3). Recently, Gilbert and Hou have studied the chemoselectivity of the [2+2] cycloaddition of cyclopentyne **1** to dihydropyran (**5**) and cyclohexene (**6**; see Scheme 4).[7] The ratio 3.3:1 (**7**:**8**) suggests a preference for the reaction of **1** with the electron-rich alkene **5**.

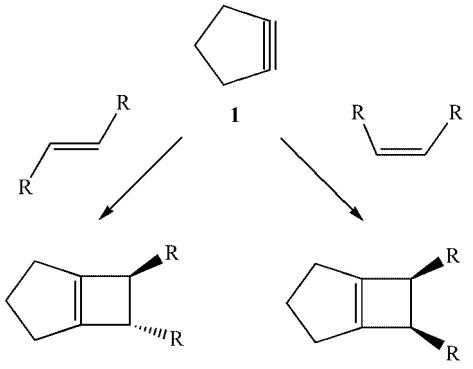

Scheme 1.

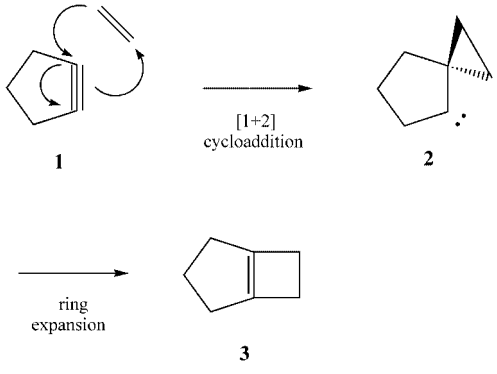

Scheme 2.

α-Methoxybenzyne undergoes several regioselective reactions like nucleophilic additions,[8,9] [2+4] cycloadditions,[10] and [2+2] cycloadditions.[11–14] Recently, Suzuki et al.[15] have reported the [2+2] cycloaddition of the benzyne **9**, which possesses a fused four-membered ring, with the ketene silyl acetal **10** to yield the cycloadducts **11** and **12** with high regioselectivity (31:1; see Scheme 5). They proposed a

[a] Instituto de Ciencia Molecular, Unidad de Investigación de Química Orgánica Teórica, Universidad de Valencia,
Dr. Moliner 50, 46100 Burjassot, Valencia, Spain
E-mail: domingo@utopia.uv.es
[b] Departamento de Ciencias Químicas, Facultad de Ecología y Recursos Naturales, Universidad Andrés Bello,
República 275, Santiago, Chile
[c] Departamento de Química, Facultad de Ciencias, Universidad de Chile,
Casilla 653, Santiago, Chile

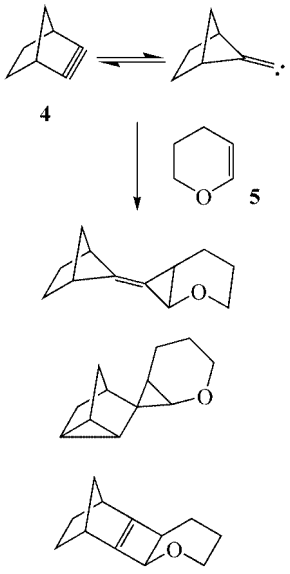

Scheme 3.

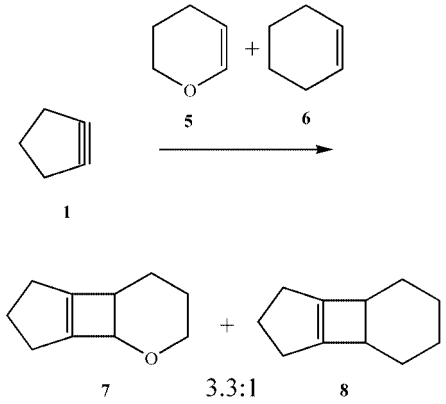

Scheme 4. Chemoselectivity in [2+2] cycloadditions of cyclopentyne

Gilbert-like mechanism for this [2+2] cycloaddition but with some zwitterionic character.[15]

Gilbert's mechanism for the [2+2] cycloaddition of cyclopentyne to ethylene has been computationally studied by Bachrach et al. at the UB3LYP and CASSCF levels of theory (see Scheme 6).[5,16] While the UB3LYP calculations pointed to a concerted pathway, the CASSCF results were more consistent with a biradical one.[16] Ozkan et al. have recently studied the [2+2] cycloadditions of cyclopentyne and benzyne to ethylene at the UB3LYP and CASSCF levels.[17] For benzyne, the biradical pathway was computed to be about 4.1 kcal mol^{-1} lower in energy than that of the concerted one involving a [1+2] cycloaddition.

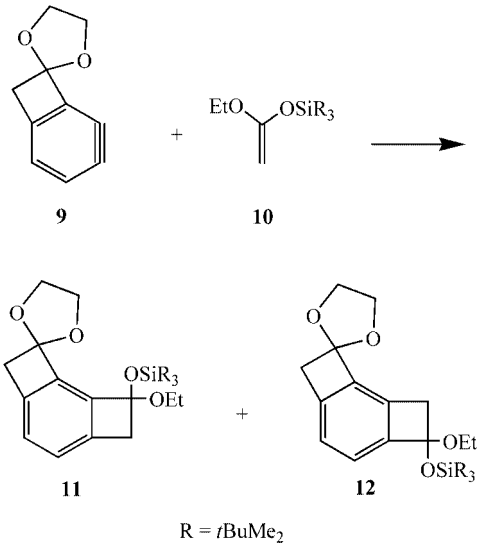

Scheme 5.

For a long time we have been interested in the study of the molecular mechanism of cycloaddition reactions. These studies have shown that the feasibility of these processes is closely associated with the polarity of the reactants.[18–20] Recently, we reported the use of the global electrophilicity index, ω, proposed by Parr et al.,[21] to classify the global electrophilicity of a series of dienes and dienophiles currently present in Diels–Alder reactions.[22] A good correlation was found between the difference in electrophilicity for the reagents, $\Delta\omega$, and the charge transfer at the corresponding transition structure (TS). This reactivity model has been further extended to 1,3-dipolar cycloadditions[23] and [4+3] cycloadditions.[24]

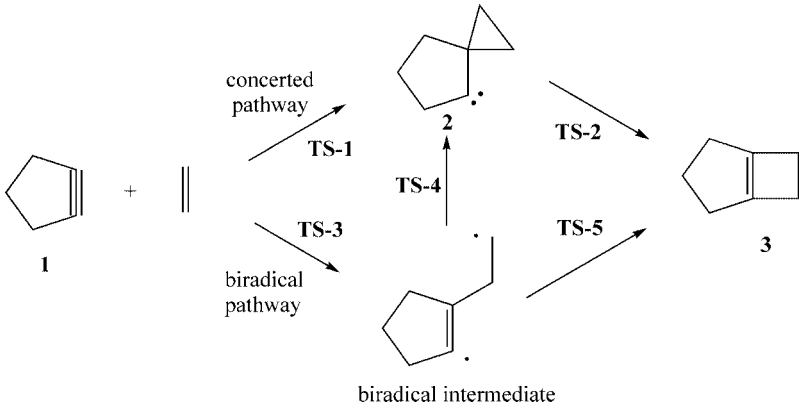

Scheme 6.

More recently, we reported a density functional theory (DFT) study of the regioselectivity of the [2+2] cycloaddition of the benzyne **13** (see Scheme 7).[25] These formal [2+2] cycloadditions are stepwise processes characterized by the nucleophilic attack of the less-substituted position of the ketene acetal **14** to the C1 position of the substituted benzyne to give a zwitterionic intermediate **IN-m**, followed by a ring-closure process to yield the corresponding [2+2] cycloadduct **15** (see Scheme 7). The first and rate-limiting step has an activation free-energy of 6.6 kcal mol^{-1}. This value is 3.2 kcal mol^{-1} lower in energy than that associated with the [1+2] cycloaddition of Gilbert's mechanism for the reaction between cyclopentyne and ethylene at the same level of theory.[5] An analysis based on the DFT reactivity indexes suggested the participation of benzyne in a polar cycloaddition. The electrophilicity of benzyne is 1.95 eV, a value that falls within the range of strong electrophiles in the ω scale.[22] This value, which is larger than that evaluated for acetylene (ω = 0.54 eV), allows us to explain the reactivity of benzyne derivatives toward nucleophilic additions. On the other hand, the ketene acetals **10** and **14** have very low electrophilicity values (ω = 0.24 and 0.26 eV, respectively) and we will assume that they behave as strong nucleophiles. The difference in electrophilicity for the benzyne/ketene acetal reaction, $\Delta\omega \approx 1.7$ eV, is in clear agreement with the charge transfer found along the cycloaddition pathway.[25]

While the analysis of reactivity (global and local) performed by means of the electrophilicity indexes has been normally treated in terms of the change in the reactivity patterns induced by suitable chemical substitution, the present study offers an interesting way of looking at electrophilic activation promoted by a less-classical substituent effect induced, for instance, by molecular strain. From a theoretical point of view, this is the first example of global or local activation in molecules induced by effects that are directly related to the external potential. The aim of the present work is to perform a DFT study of the strain-induced electrophilicity of the cycloalkynes and bicycloalkynes series given in Scheme 8. The polar [2+2] cycloaddition between cyclopentyne (**1**) and methyl vinyl ether (**16**) will be analyzed in order to understand the reactivity of cyclopentyne toward nucleophilic attacks (see Scheme 9).

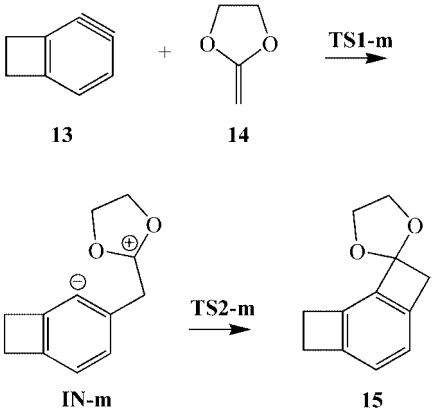

Scheme 7.

Results and Discussion

Cycloalkynes are strained molecules that show a large deviation of the internal ring angle from the linear disposition of the C^{sp^3}–C^{sp}–C^{sp} atoms. The strain in small cycloalkynes has been theoretically evaluated by Johnson and Daoust[26] using MP2/6-31G* energies through the isodesmic reactions shown in Figure 1. The π-strain (S_π, hereafter) for cyclohexyne (C6), cyclopentyne (C5), and cyclobutyne (C4), was estimated to be 40.7, 69.5, and 74.6 kcal mol^{-1}, respectively.[26]

We have evaluated the S_π quantity for the series of cycloalkynes C5–C8, including benzyne (Bz), and the series of bicycloalkynes BC211, BC221, and BC222 shown in Scheme 8, at the B3LYP/6-31G* level and using the same isodesmic reaction used by Johnson and Daoust[26] (see Figure 1). The energy results are summarized in Table 1. An analysis of ΔE_{iso} values shows an increase of the π-strain with the reduction of the ring size, from an eight- to a five-membered ring. The ΔE_{iso} values obtained at this DFT level for C5 and C6 are, within a range of 3–5 kcal mol^{-1}, higher in energy than those obtained using MP2 calculations.[26]

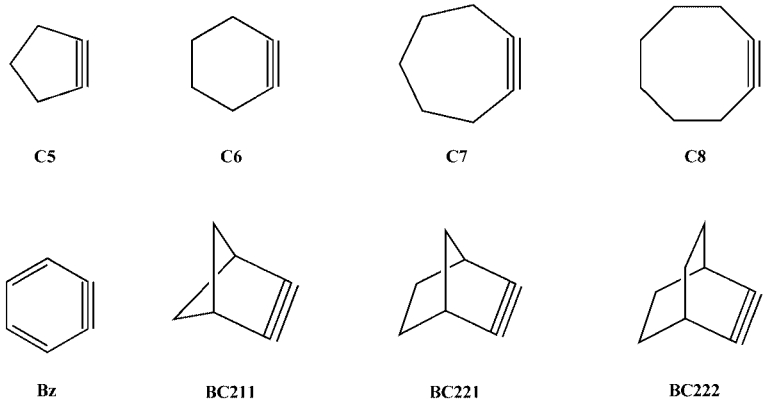

Scheme 8.

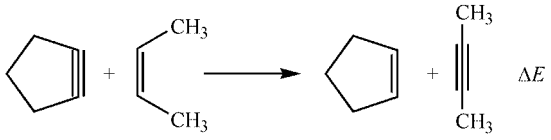

Figure 1. Isodesmic reaction model used to evaluate molecular strain in the cycloalkyne series.

Table 1. B3LYP/6-31G* total energies of cycloalkynes and cycloalkenes (E_1 and E_2, respectively, in au) and energies for the isodesmic reaction shown in Figure 1 (ΔE_{iso}, in kcal mol^{-1}). IBA is the internal C–C–C bond angle of cycloalkynes (in degrees).[a]

	E_1	E_2	ΔE_{iso}	IBA
BC211	–231.994565	–233.364979	78.19	105.3
C5	–193.962864	–195.326701	74.06	115.9
BC221	–271.366361	–272.727383	72.30	110.4
Bz	–230.909948	–232.248652	58.29	127.1
BC222	–310.720693	–312.056681	56.59	119.5
C6	–233.332556	–234.648288	43.88	131.4
C7	–272.659614	–273.950310	28.17	142.3
C8	–311.995054	–313.254684	8.67	153.8

[a] The total energies of *cis*-2-butene and 2-butyne are –157.224769 and –155.978961 au, respectively.

A plot of the π-strain energy measured by ΔE_{iso} vs. the deviation of the internal bond angle from the linear geometry (*DIBA* = 0° is the reference value) allows us to obtain a good linear eight-point correlation, with a regression coefficient, R^2, of 0.96. The resulting regression is shown in Equation (1); see also Figure 2.

$$S_\pi = 1.455 \times DIBA - 26.488 \quad (1)$$

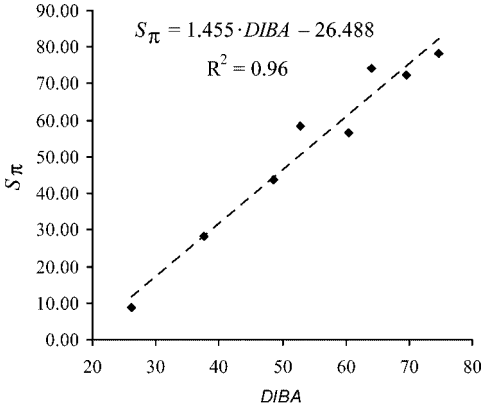

Figure 2. Plot of π-strain (S_π) [kcal mol^{-1}] vs. the deviation of the internal bond angle (*DIBA*, in degrees) for the complete series of cycloalkynes.

Some deviations can be related to the structural variations of the cycloalkynes. For instance, cyclohexyne (C6), benzyne (Bz), and bicyclo[2,2,2]oct-2-yne (BC222), which have a six-membered cycloalkyne ring, have different structural features, such as the planar ring in the case of benzyne and the presence of a second ring in the case of the bicyclic system. In fact, if we consider the sub-series C5, C6, C7, and C8, the regression coefficient improves to $R^2 = 0.99$.

The π-strain in cycloalkynes has been rationalized by Johnson and Daoust.[26] If a double bond is twisted, the limit of S_π should be the rotational barrier (ca. 65 kcal mol^{-1}). This energy can be associated to the breaking of the π bond to form a perpendicular biradical species. By analogy, there should also be a limit to S_π in alkynes, which would be attained for the in-plane bending (i.e. a π-bond strength of 76 kcal mol^{-1}). This energy can also be associated to the breaking of the π bond located in the carbocycle plane, thus suggesting some biradical character for the small cycloalkynes. Thus, CASSCF(4,4)/6-31G* calculations yield a biradical character of 10% for C5. Note that our DFT energy for BC211 is slightly larger than this value as a consequence of the large strain associated with the [2.1.1] bicyclic system.

Now the question is: is there any relationship between S_π and the electrophilicity of the cycloalkyne series? Recently, we have shown that the reactivity of benzyne derivatives containing strained substituents toward nucleophile reagents can be consistently explained by their π-strain-enhanced electrophilicities.[25] In order to further explore a more general relationship between π-strain and the electrophilicity, the electrophilicity index of the cycloalkynes C5–C8, Bz, and the bicycloalkynes BC211, BC221, and BC222 were computed. They are compiled in Table 2, which also includes the corresponding values of the electronic chemical potential, μ, and the chemical hardness, η. Acetylene and 2-butyne are also incorporated as reference compounds.

Table 2. HOMO and LUMO energies (in au), electronic chemical potential (μ, in au), chemical hardness (η, in au), and global electrophilicity (ω, in eV) for the cycloalkynes and bicycloalkynes series.

	HOMO	LUMO	μ	η	ω
BC211	–0.2344	–0.1041	–0.1693	0.1303	2.99
BC221	–0.2351	–0.0904	–0.1627	0.1447	2.49
C5	–0.2353	–0.0886	–0.1620	0.1467	2.43
Bz	–0.2584	–0.0701	–0.1643	0.1883	1.95
BC222	–0.2363	–0.0633	–0.1498	0.1730	1.76
C6	–0.2317	–0.0338	–0.1327	0.1979	1.21
C7	–0.2311	–0.0038	–0.1174	0.2273	0.83
C8	–0.2338	0.0270	–0.1034	0.2607	0.56
HC≡CH	–0.2819	0.0524	–0.1148	0.3344	0.54
$CH_3C{\equiv}CCH_3$	–0.2406	0.0680	–0.0863	0.3086	0.33

Benzyne has a global electrophilicity value of 1.95 eV,[25] and it may be classified as a strong electrophile within the electrophilicity scale.[22] It undergoes nucleophilic addition reactions.[8,9] On the other hand, cyclohexyne has an electrophilicity value of 1.21 eV, which corresponds to a moderate electrophile in the theoretical scale of electrophilicity.[22] Note that 2-butyne has an electrophilicity value of 0.33 eV, and therefore it may be classified as a marginal electrophile, or nucleophile. Cyclopentyne has an electrophilicity value that is larger than benzyne (2.43 eV). Therefore, it is expected to react as an electrophile toward good nucleophiles in a polar process. The sub-series of bicycloalkynes BC211, BC221, and BC222 also presents enhanced electrophilicity patterns (1.76, 2.49, and 2.99 eV, respectively), which may be related to the π-strain present in these bicyclic systems.

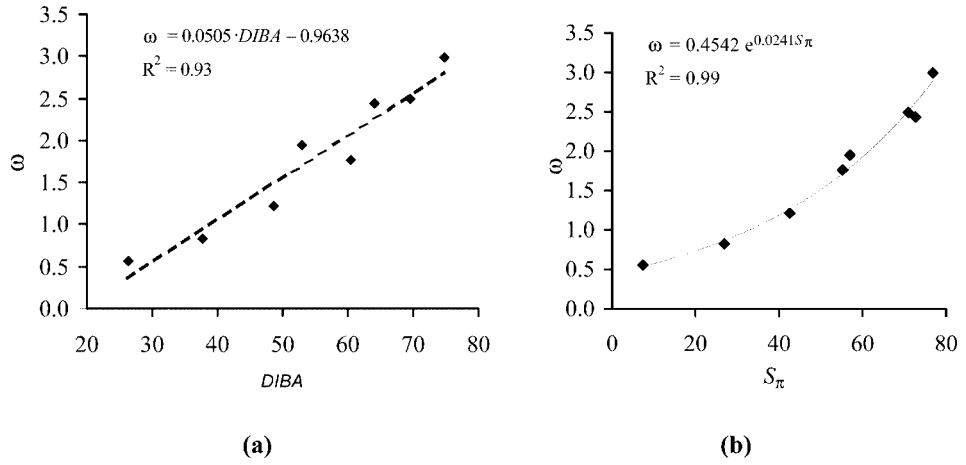

Figure 3. Plots of the electrophilicity index, ω [eV], vs. (a) the deviation of the internal bond angle (*DIBA*, in degrees) and (b) π-strain (S_π) [kcal mol^{-1}] for the complete series of cycloalkynes.

We have performed a statistical analysis by quantitatively comparing the electrophilicity index of these cycloalkynes and the *DIBA*s. The results are summarized in Figure 3 (a). A good, linear eight-point correlation between the electrophilicity, ω, and *DIBA* is found (R^2 = 0.93). The resulting regression is shown in Equation (2).

$$\omega = 0.0505 \times DIBA - 0.9638 \quad (2)$$

A better correlation can be obtained when the electrophilicity of these cycloalkynes is plotted against the S_π index. These results are summarized in Figure 3 (b). In this case the correlation is even better (R^2 = 0.99), although the relationship is no longer linear but exponential.

We may wonder now what is the origin of this electrophilic activation induced by π-strain. Electrophilicity is a kinetic concept that, in the cases of alkenes and alkynes, can be related to the easy formation of the corresponding carbanion that results from a nucleophilic attack to the π-bond. Unsubstituted acyclic alkynes do not act as electrophiles because of the large destabilization of the corresponding vinyl carbanion. For small cycloalkynes, however, the π-strain destabilizes the ground state, thereby decreasing the energy gap relative to the corresponding carbanion.[27] In summary, the π-strain induces electrophilic activation on small cycloalkynes. The electrophilicity of these compounds is correctly represented by a linear correlation with the DIBA given by Equation (2). Small cycloalkynes present larger electrophilicity values, and therefore they are expected to react efficiently with strong nucleophiles through a polar interaction.

In order to test this prognosis we studied the polar [2+2] cycloaddition between cyclopentyne (**1**) and methyl vinyl ether (**16**, see Scheme 9) as a model for the [2+2] cycloaddition between **1** and dihydropyran (**5**, see Scheme 4).[7] Recently, we have shown that the regioselectivity in the [2+2] cycloaddition of the benzyne **9** to ketene acetals can be correctly explained by a polar process characterized by the nucleophilic attack of the ketene acetal **14** to the substituted benzyne **13** (see Scheme 7).[25] Cyclopentyne has a larger electrophilicity value than benzyne, and therefore it is expected to react with nucleophiles such as **16** in a polar process.

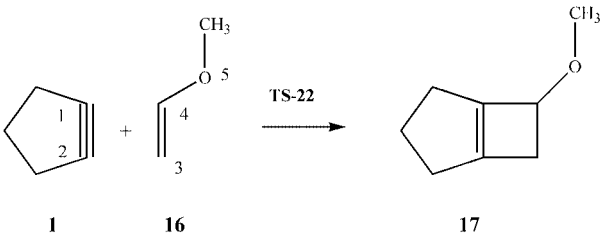

Scheme 9.

At the B3LYP/6-31G* level, the reaction between **1** and **16** presents a barrierless pathway directly connecting with the [2+2] cycloadduct **17**. An exploration of the PES at the MP2/6-31G* level allowed us to locate a transition structure, **TS-22**, connecting the reactants with the corresponding cyclobutene **17** (see Scheme 9). The geometry of **TS-22** is given in Figure 4 (a). The energy results are summarized in Table 3. The activation enthalpy associated with **TS-22** is 5.6 kcal mol^{-1}. CASSCF(4,4)/6-31G*//MP2/6-31G* calculations confirmed the closed-shell configuration of this TS, thereby allowing us to discard a biradical character.[5,16] The IRC calculations show that the reaction channel directly connects this transition structure with the cyclobutene **17**. The IRC plot is shown in Figure 5. The analysis of the IRC shows that this cycloaddition is a two-stage process.[28] In the first step, the C2–C3 bond is completely formed along the nucleophilic attack of the nonsubstituted position of the double bond of **16** to one carbon atom of the triple C≡C bond of cyclopentyne; the C1–C4 bond is formed in the second stage. From the IRC analysis we have selected the inflexion point of the IRC (IRC-IP) that shares the reaction coordinates in the two stages. Note that this point on the IRC is not a stationary point; the IRC-IP is located 23.0 kcal mol^{-1} below the reactants. However, the absence of any appreciable barrier for the ring-closure precludes the IRC-IP from becoming a stationary point on the PES, and as a result the mechanism is characterized by a

Table 3. Total (in au) and relative[a] (in kcal mol^{-1}) energies (E and ΔE; ΔE_{sol} are the relative energies in dichloromethane), enthalpies (H and ΔH), and free energies (G and ΔG) (computed at 25 °C and 1 atm) of the stationary points for the polar [2+2] cycloaddition between **1** and **16**, and the [1+2] cycloaddition between **1** and ethylene.

	E	ΔE	ΔE_{sol}	H	ΔH	G	ΔG
1	–193.299650			–193.197415		–193.229324	
16	–192.471204			–192.379872		–192.411499	
TS-22	–385.761135	6.10	5.82	–385.568360	5.60	–385.617570	14.59
17	–385.915040	–90.48	–88.93	–385.717210	–87.80	–385.760570	–75.14
Ethylene	–78.285028			–78.229009		–78.253866	
TS-12	–271.568243	10.31	8.97	–271.411730	9.22	–271.453296	18.76
2	–271.644641	–37.63	–37.89	–271.484818	–36.64	–271.522160	–24.45
3	–271.729512	–90.88	–89.45	–271.567681	–88.64	–271.604730	–76.27

[a] Relative to **1** + **16** and **1** + ethylene.

highly asynchronous concerted process.[28] Despite the zwitterionic character of IRC-IP, the loss of the π-strain is responsible for its large stabilization. The cycloaddition is strongly exothermic (–87.8 kcal mol^{-1}), and an important part of this energy (ca. 70 kcal mol^{-1}) is due to the absence of π-strain in the cyclopentene.

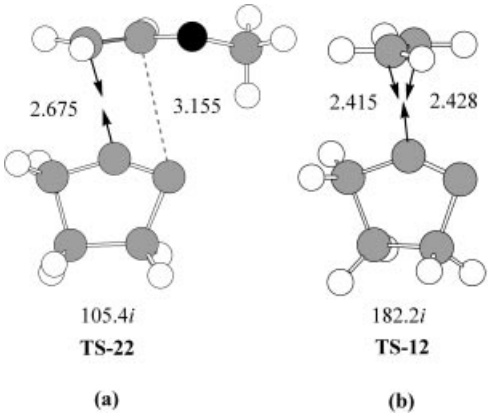

Figure 4. MP2/6-31G* geometries of the transition structures involved in (a) the [2+2] cycloaddition between **1** and **16** (**TS-22**), and (b) the [1+2] cycloaddition between **1** and ethylene (**TS-12**). The distances are given in angstroms. The unique imaginary frequencies (in cm^{-1}) and the corresponding displacement vectors are also given.

In order to compare the energy barrier associated with the polar [2+2] cycloaddition between **1** and **16** with that corresponding to the formation of the spirocarbene **2**, the TS associated with the [1+2] cycloaddition between **1** and ethylene was also studied (**TS-12** in Scheme 10). At the MP2/6-31G* level **TS-12** is located 9.2 kcal mol^{-1} above the reagents. Therefore, the activation enthalpy for the polar [2+2] cycloaddition between **1** and **16** is 3.6 kcal mol^{-1} lower in energy than that associated with the [1+2] cycloaddition between **1** and ethylene. This result is in agreement with the experimentally observed chemoselectivity in the [2+2] cycloaddition of **1** to **5** and **6** (see Scheme 4 and ref.[7]), and further supports our assertion that the polar mechanism is preferred over the nonpolar one when electrophilic and nucleophilic species are interacting. [Note that cyclopentyne is classified as a strong electrophile while ethylene is classified as a moderate electrophile (ω = 0.73 eV)[22] i.e. a weak nucleophile.] In consequence, the cycloaddition between **1** and ethylene will take place along a nonpolar process through pericyclic or stepwise biradical mechanisms.[5,16] On the other hand, the use of more nucleophilic reagents than **16**, such as the ketene acetals **10** and **14** or enamines – the electrophilicity of dimethyl vinyl amine is 0.27 eV[22] – will favor a polar mechanism.

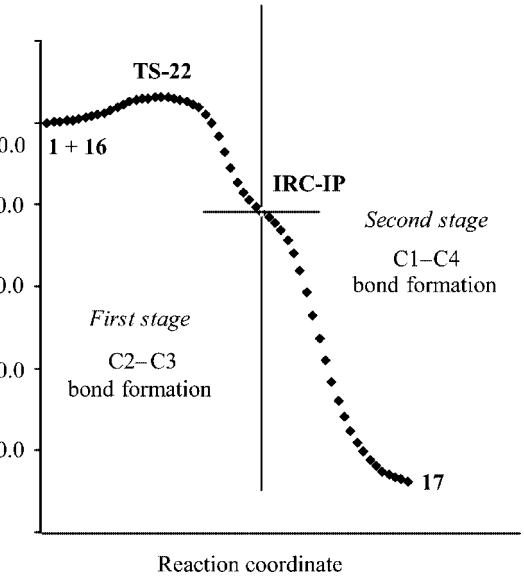

Figure 5. MP2/6-31G* reaction profile for the two-stage, one-step [2+2] cycloaddition between **1** and **16**. IRC-IP corresponds to the inflexion point on the IRC that shares the two-stage regions.

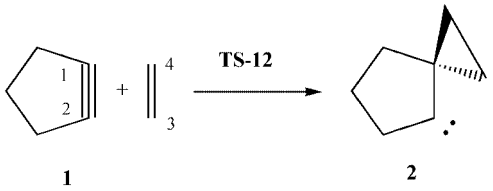

Scheme 10.

The bond lengths between the carbon atoms involved in the C–C bond formation along these cycloaddition processes are given in Figure 4. The length of the C2–C3 forming bond at **TS-22** is 2.675 Å, while the distance between the C1 and C4 centers is 3.155 Å (Figure 4, a). These geometrical parameters indicate that this TS is very early, a

result consistent with the low barrier and the strong exothermic character of the cycloaddition.[27] The length of the C1–C3 and C1–C4 forming bonds at **TS-12** are 2.415 and 2.428 Å, respectively (Figure 4, b). These distances are slightly shorter than those found at the B3LYP/6-31G* level.[5]

At the IRC-IP stage the length of the C2–C3 bond is 1.529 Å, while the distance between the C1 and C4 centers remains at 2.932 Å (see Figure 6). The IRC-IP structurally and electronically resembles the zwitterionic intermediate IN-m found along the [2+2] cycloaddition between the benzyne **13** and the ketene acetal **14** (see Scheme 7).[25]

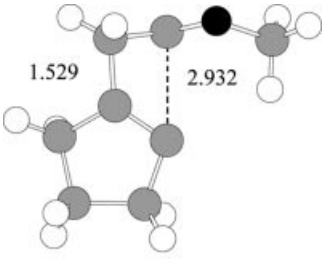

Figure 6. MP2/6-31G* geometry of the inflexion point IRC-IP on the IRC between **TS-22** and the [2+2] cycloadduct **17**. The bond lengths between the atoms directly involved in the reaction are given in angstroms.

The analysis of the atomic motion associated with the unique imaginary frequency of the **TS-22**, $105.4\,i\,cm^{-1}$, indicates that this TS is mainly associated with the displacement of the C2 and C3 atoms along the C2–C3 bond formation. The movement of the C1 and C4 atoms is negligible. Therefore, both the geometrical and vibrational analysis at the **TS-22** are consistent with a two-center addition. A different behavior is found at **TS-12** (ν = $182.2\,i\,cm^{-1}$), where the bond formation process is associated with the symmetric displacement of the ethylene C3 and C4 atoms and the cyclopentyne C1 atom along the C1–C3 and C1–C4 bond formation. A schematic representation of these vibrations at both TSs is given in Figure 4.

The natural population analysis (NPA) allows us to evaluate the charge transfer (CT) along the nucleophilic attack of methyl vinyl ether to cyclopentyne. The natural charges at **TS-22** appear to be shared between the donor methyl vinyl ether and the acceptor cyclopentyne. The CT at **TS-22** is 0.07 e, while at the IRC-IP stage the CT presents a larger value (0.53 e). This value is slightly larger than that found at the zwitterionic intermediate **IN-m**,[25] and stresses the polar character of this formal [2+2] cycloaddition. The charge transfer at the IRC-IP is, in turn, consistent with the large $\Delta\omega$ value found for the cyclopentyne + methyl vinyl ether reaction. At **TS-12** the CT is 0.15 e, while at the [1+2] cycloadduct **2** it is 0.18 e. The larger CT found at **TS-12** than at **TS-22** is a consequence of the early character of **TS-22**. However, along the polar [2+2] cycloaddition the CT increases to the IRC-IP stage.

Finally, the solvent effects of dichloromethane have been modeled using the PCM method. Table 3 reports the relative energies. Solvent effects stabilize all stationary points between 0.3 and 4.4 $kcal\,mol^{-1}$. **TS-22** and **TS-12** are stabilized by 3.35 and 3.07 $kcal\,mol^{-1}$. These small differences are due to the early character of **TS-22**. However, IRC-IP is 2.42 $kcal\,mol^{-1}$ more stabilized than the [1+2] cycloadduct **2**, due to the large zwitterionic character of the former. The activation barriers for these cycloadditions are 5.82 (**TS-22**) and 8.97 $kcal\,mol^{-1}$ (**TS-12**). In dichloromethane, the barrier for the formation of the [2+2] cycloadduct **17** remains 3.16 $kcal\,mol^{-1}$ below the barrier for the formation of the [2+1] cycloadduct **2**.

Conclusions

The reactivity of strained cycloalkynes participating in a polar reaction has been studied using the electrophilicity index. A good correlation between the strain angle and the electrophilicity index is found for cycloalkynes. Thus, the large electrophilicity values of cyclopentyne and benzyne allow us to explain their reactivity toward nucleophiles. In order to test this reactivity model, the [2+2] cycloaddition between cyclopentyne and methyl vinyl ether has been studied. An analysis based on the bond formation along this cycloaddition indicates that this reaction is a highly asynchronous concerted process characterized by the nucleophilic attack of methyl vinyl ether to the cyclopentyne acting as a good electrophile. The polar character of this cycloaddition is in clear agreement with the large $\Delta\omega$ value found for the cyclopentyne + methyl vinyl ether reaction.

This polar mechanism may be considered as a reliable alternative to those proposed by Gilbert for the cyclopentyne/ethylene reaction, with one initiated by a [1+2] cycloaddition to give a spirocarbene intermediate,[5] and the other one leading to a biradical stepwise [2+2] cycloaddition.[16] The electrophilicity index indicates that cyclopentyne and benzyne are strong electrophiles, and that they may participate in polar reactions in the presence of electron-rich alkenes. In the absence of these species, carbene or biradical mechanisms can be operative. This result is in agreement with the chemoselective [2+2] cycloadditions of cyclopentyne to the electron-rich dihydropyran and cyclohexene.[7]

Experimental Section

The Electrophilicity Index

The global electrophilicity index, ω, which measures the stabilization in energy when the system acquires an additional electronic charge, ΔN, from the environment, is given by the simple expression in Equation (3),[21]

$$\omega = \frac{\mu^2}{2\eta} \tag{3}$$

in terms of the electronic chemical potential, μ, and the chemical hardness, η. Both quantities may be approached in terms of the one-electron energies of the frontier molecular orbitals HOMO and LUMO (ε_H and ε_L, respectively) as $\mu \approx (\varepsilon_H + \varepsilon_L)/2$ and $\eta \approx \varepsilon_L - \varepsilon_H$, respectively.[29] The electrophilicity index encompasses both the propensity of the electrophile to acquire an additional electronic charge [driven by μ^2 (the square of electronegativity) $\chi = -\mu$] and the resistance of the system to exchange electronic charge with the environment, described by η. A good electrophile is, in this sense, characterized by high values of electronegativity and softness.

Computational Data

Calculations were carried out using the B3LYP[30,31] exchange-correlation functionals, and the MP2 theory levels,[32] together with the standard 6-31G* basis set,[32] which has recently been used in the study of related [2+2] cycloadditions of small cycloalkynes.[5,16,25] The optimizations were performed using the Berny analytical gradient optimization method.[33,34] The stationary points were characterized by frequency calculations in order to verify that the transition structures had one, and only one, imaginary frequency. The intrinsic reaction coordinate (IRC)[35] path was traced in order to check that the energy profiles connected each transition structure to the two associated minima of the proposed mechanism, by using the second-order González–Schlegel integration method.[36,37] The stability of the RMP2/6-31G* wavefunctions was tested using the keyword stable = opt at the UMP2/6-31G* level. All wavefunctions were stable under the perturbations considered, and they gave the same results as those obtained at the RMP2/6-31G* level. The values of the enthalpies and free energies were calculated based on the total energies and the thermochemical analysis at the MP2/6-31G* level.[32] These energies were computed at 25 °C and 1 atm. The electronic structures of stationary points were analyzed by the natural bond orbital (NBO) method.[38,39] All calculations were carried out using the Gaussian 98 suite of programs.[40]

The solvent effects of dichloromethane, modeled as a continuum model, were considered by HF/6-31G* single-point calculations at the gas-phase-optimized geometries using a self-consistent reaction field (SCRF)[41–42] based on the polarizable continuum model (PCM) of Tomasi's group.[43–45] The electronic energies in solution, $E_{CH_2Cl_2}$, were obtained by adding the total electrostatic energies obtained from the PCM calculations to the electronic energies in vacuo. The PCM and solvent = dichloromethane options were employed in the SCRF calculations.

Acknowledgments

This work received partial financial support from the Ministerio de Educación y Cultura of the Spanish Government by DGICYT (BQU2002-01032), the Agencia Valenciana de Ciencia y Tecnología of the Generalitat Valenciana (reference GRUPOS03/176), and Fondecyt (grants 1020069 and 1030548). P. P. thanks DI-UNAB-17-04. L. R. D. thanks Fondecyt (grant no. 7020069) for financial support and the Universidad Andrés Bello (Chile) for their warm hospitality. The authors acknowledge the Millennium Nucleus for Applied Quantum Mechanics and Computational Chemistry, grant (P02-004-F, MIDEPLAN-CONICYT).

[1] L. Fitjer, S. Modaressi, *Tetrahedron Lett.* **1983**, *24*, 5495.
[2] J. C. Gilbert, M. E. Baze, *J. Am. Chem. Soc.* **1984**, *106*, 1885.
[3] R. B. Woodward, R. Hoffmann, *The Conservation of Orbital Symmetry*, Verlag Chemie, Weinheim, **1970**.
[4] I. Fleming, *Frontier Orbitals and Organic Chemical Reactions*, John Wiley & Sons, New York, **1976**.
[5] S. M. Bachrach, J. C. Gilbert, D. W. Laird, *J. Am. Chem. Soc.* **2001**, *123*, 6706.
[6] D. W. Laird, J. C. Gilbert, *J. Am. Chem. Soc.* **2001**, *123*, 6704.
[7] J. C. Gilbert, D.-R. Hou, *J. Org. Chem.* **2003**, *68*, 10067.
[8] R. Huisgen, H. Rist, *Justus Liebigs Ann. Chem.* **1955**, *594*, 137.
[9] R. A. Benkeser, C. E. DeBoer, *J. Org. Chem.* **1956**, *21*, 281.
[10] T. Matsumoto, T. Hosoya, M. Katsuki, K. Suzuki, *Tetrahedron Lett.* **1991**, *32*, 6735.
[11] T. Hosoya, T. Hasegawa, Y. Kuriyama, T. Matsumoto, K. Suzuki, *Synlett* **1995**, 177.
[12] T. Hosoya, T. Hasegawa, Y. Kuriyama, K. Suzuki, *Tetrahedron Lett.* **1995**, *36*, 3377.
[13] T. Hosoya, T. Hamura, Y. Kuriyama, K. Suzuki, *Synlett* **2000**, 520.
[14] T. Hamura, T. Hosoya, H. Yamaguchi, Y. Kuriyama, M. Tanabe, M. Miyamoto, Y. Yasui, T. Matsumoto, K. Suzuki, *Helv. Chim. Acta* **2002**, *85*, 3589.
[15] T. Hamura, Y. Ibusuki, K. Sato, T. Matsumoto, Y. Osamura, K. Suzuki, *Org. Lett.* **2003**, *5*, 3551.
[16] S. M. Bachrach, J. C. Gilbert, *J. Org. Chem.* **2004**, *69*, 6357.
[17] I. Ozkan, A. Kinal, *J. Org. Chem.* **2004**, *69*, 5390.
[18] L. R. Domingo, M. Arnó, J. Andrés, *J. Org. Chem.* **1999**, *64*, 5867.
[19] L. R. Domingo, *Tetrahedron* **2002**, *58*, 3765.
[20] L. R. Domingo, M. J. Aurell, P. Pérez, R. Contreras, *J. Org. Chem.* **2003**, *68*, 3884.
[21] R. G. Parr, L. von Szentpaly, S. Liu, *J. Am. Chem. Soc.* **1999**, *121*, 1922.
[22] L. R. Domingo, M. J. Aurell, P. Pérez, R. Contreras, *Tetrahedron* **2002**, *58*, 4417.
[23] P. Pérez, L. R. Domingo, M. J. Aurell, R. Contreras, *Tetrahedron* **2003**, *59*, 3117.
[24] J. A. Sáez, M. Arnó, L. R. Domingo, *Org. Lett.* **2003**, *5*, 4117.
[25] L. R. Domingo, P. Pérez, R. Contreras, *Lett. Org. Chem.* **2005**, *2*, 68.
[26] R. P. Johnson, K. J. Daoust, *J. Am. Chem. Soc.* **1995**, *117*, 362.
[27] G. S. Hammond, *J. Am. Chem. Soc.* **1955**, *77*, 334.
[28] L. R. Domingo, *J. Org. Chem.* **2001**, *66*, 3211.
[29] R. G. Parr, W. Yang, *Density Functional Theory of Atoms and Molecules*, Oxford University Press, New York, **1989**.
[30] A. D. Becke, *J. Chem. Phys.* **1993**, *98*, 5648.
[31] C. Lee, W. Yang, R. G. Parr, *Phys. Rev. B* **1988**, *37*, 785.
[32] W. J. Hehre, L. Radom, P. v. R. Schleyer, J. A. Pople, *Ab initio Molecular Orbital Theory*, Wiley, New York, **1986**.
[33] H. B. Schlegel, *J. Comput. Chem.* **1982**, *3*, 214.
[34] H. B. Schlegel, *Geometry Optimization on the Potential Energy Surface*, in *Modern Electronic Structure Theory* (Ed.: D. R. Yarkony), World Scientific Publishing, Singapore, **1994**.
[35] K. Fukui, *J. Phys. Chem.* **1970**, *74*, 4161.
[36] C. González, H. B. Schlegel, *J. Phys. Chem.* **1990**, *94*, 5523.
[37] C. González, H. B. Schlegel, *J. Chem. Phys.* **1991**, *95*, 5853.
[38] A. E. Reed, R. B. Weinstock, F. Weinhold, *J. Chem. Phys.* **1985**, *83*, 735.
[39] A. E. Reed, L. A. Curtiss, F. Weinhold, *Chem. Rev.* **1988**, *88*, 899.
[40] M. J. Frisch, G. W. Trucks, H. B. Schlegel, G. E. Scuseria, M. A. Robb, J. R. Cheeseman, V. G. Zakrzewski, J. A. Montgomery Jr., R E. Stratmann, J. C. Burant, S. Dapprich, J. M. Millam, A. D. Daniels, K. N. Kudin, M. C. Strain, O. Farkas, J. Tomasi, V. Barone, M. Cossi, R. Cammi, B. Mennucci, C. Pomelli, C. Adamo, S. Clifford, J. Ochterski, G. A. Petersson, P. Y. Ayala, Q. Cui, K. Morokuma, D. K. Malick, A. D. Rabuck, K. Raghavachari, J. B. Foresman, J. Cioslowski, J. V. Ortiz, B. B. Stefanov, G. Liu, A. Liashenko, P. Piskorz, I. Komaromi, R. Gomperts, R. L. Martin, D. J. Fox, T. Keith, M. A. Al-Laham, C. Y. Peng, A. Nanayakkara, M. Challacombe, P. M. W. Gill, B. Johnson, W. Chen, M. W. Wong, J. L. Andres, C. Gonzalez, M. Head-Gordon, E. S. Replogle, J. A. Pople,

Gaussian 98, Revision A.6, Gaussian, Inc., Pittsburgh, PA, **1998**.
[41] J. Tomasi, M. Persico, *Chem. Rev.* **1994**, *94*, 2027.
[42] B. Y. Simkin, I. Sheikhet, *Quantum Chemical and Statistical Theory of Solutions − A Computational Approach*, Ellis Horwood, London, **1995**.
[43] M. Cossi, V. Barone, R. Cammi, J. Tomasi, *Chem. Phys. Lett.* **1996**, *255*, 327.
[44] E. Cances, B. Mennuncci, J. Tomasi, *J. Chem. Phys.* **1997**, *107*, 3032.
[45] V. Barone, M. Cossi, J. Tomasi, *J. Comp. Chem.* **1998**, *19*, 404.